# A SYSTEM FOR THE AUTOMATIC DETECTION OF PIGMENT NETWORK

*Catarina Barata, Jorge S. Marques*

Institute for Systems and Robotics
Instituto Superior Técnico
Portugal

*Jorge Rozeira*

Hospital Pedro Hispano
Matosinhos
Portugal

**ABSTRACT**

Pigment network is considered a key differential structure by dermatologists. Recently, different approaches have been proposed for the detection and characterization of this structure. This paper proposes an improved system for automatic detection of pigment network regions. The system starts by detecting the presence of pigment network using a bank of directional filters and a connected component analysis. After, a set of features, which characterize the pigment network's lines and the background, is extracted and used to validate the detected regions with AdaBoost. Finally, each lesion is classified regarding the presence or absence of pigment network The algorithm was tested in a dataset of dermoscopy images from Hospital Pedro Hispano (Matosinhos) achieving a $SE = 78\%$ and a $SP = 77\%$ for five fold cross validation.

***Index Terms***— Melanoma, Dermoscopy, Pigment Network Detection, Directional Filters, Feature Extraction,

## 1 Introduction

Melanoma is the deadliest form of skin cancer. However, when detected in an early stage, a simple excision drastically improves the probability of survival [1]. Dermoscopy is a screening technique used by dermatologists to visualize skin lesions. Depending on the instrument used a lesion can be magnified up to 100x, which enables the observation of pigmented structures, such as pigment network, dots, streaks and coloration. These structures can then be used by dermatologists to perform a lesion classification and to assess its degree of malignancy, by recurring to one or more of the several medical procedures available ( *e.g.*, ABCD rule [2], 7-point check list [3] and Menzies method [4]) Studies proved that dermoscopy can improve the early detection of melanomas when used by an experient operator [5]. However, if the dermatologist is insufficiently trained, the accuracy of the detection decreases [6]. Moreover, since it depends greatly on the vision of the dermatologist, this method is a subjective one, lacking reproducibility.

The limitations of dermoscopy fostered the development of several computed aided diagnosis (CAD) systems, which try to perform an early detection of melanomas. A recent approach proposed in several of these systems is to try to incorporate the medical knowledge by detecting the dermoscopic features used by dermatologists such as pigment network, dots, streaks and blue white veil [7, 8, 9, 10, 11, 12, 13].

Recently, some systems for the detection of pigment network have been proposed [7, 8, 9, 10, 11]. This dermoscopic structure is considered to play a major role both in skin lesion distinction, since it is an hallmark of melanocytic lesions, and in melanoma diagnosis, since an atypical pigment network is usually an unmistakable sign of malignancy. Pigment network has a very characteristic shape, appearing as a grid of thin dark lines over a lighter background, very similar to a honeycomb. Fig. 1 exemplifies two different kinds of lesions, one where pigment network is present and other one where it is absent.

This paper proposes an improvement over the pigment network detection system proposed in [9], which uses the color and geometrical properties of pigment network to perform its detection. This system detects most of the pigment network regions in the dataset but it has a large number of false alarms. To overcome this difficulty, two novel blocks were included in this system: a region validation block, which uses a pattern recognition approach to validate the detected regions and a lesion classification block. The paper is organized as follows. Section 2 presents an overview of the proposed system. Sections 3 and 4 describe the region validation and lesion classification algorithms. Section 5 describes the performance metrics and section 6 describes an experimental evaluation of the method. Section 7 concludes the paper.

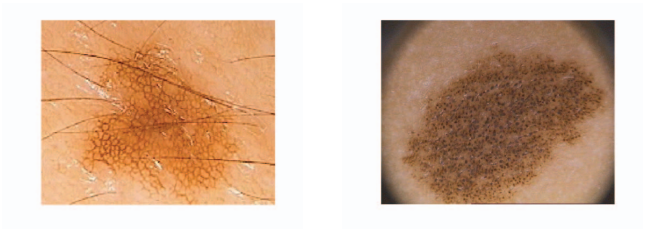


**Fig. 1:** Examples of lesions: (left) pigment network is present; (right) pigment network is absent.

This work was supported by FCT in the scope of project PTDC/SAU-BEB/103471/2008

## 2 System Overview

The detection system proposed is composed by five consecutive blocks, as in Fig. 2. The three first blocks are described in [9] whilst the last two will be discussed in the following sections.

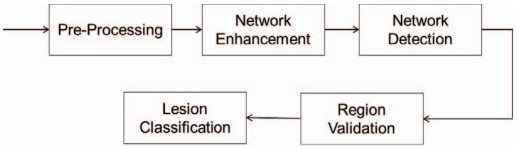



**Fig. 2:** Block Diagram of the Detection System

The first block is a pre-processing one, where two kinds of artifacts are removed: hair and reflections produced during the acquisition process. The algorithms used for hair and reflection detection and removal are the ones described in [9].

The network enhancement and detection blocks detect and extract the lines which compose the mesh of pigment network. The first block uses a bank of directional filters to perform the enhancement of the lines, while the second block makes use of a connected component analysis and an area-based thresholding to extract them, generating a binary network mask. Details can be found in [9].

The fourth block aims to reduce the false alarms and to increase the specificity. This is done by extracting several features which characterize the detected region. These features are then used to classify each region as *pigment network* or *not* by using a boosting algorithm.

The final lesion classification block performs a binary labeling of a lesion as *with* or *without pigment network*.

## 3 Region Validation

The network detection algorithm proposed in [9] tends to detect regions in excess, which means that it presents a low rate of detection failures but a high number of false alarms. The algorithm used in the network detection block is a simple one, which does not explore all the properties of pigment network. Therefore, it was decided that some region post-processing could be done to improve the detection results. A pattern recognition approach was adopted, since the decision rule would be learned from classified data. Several features which characterize the intensity, texture and topology of the region were extracted and used to train a classifier (AdaBoost [14]) to perform a binary classification. Since the output of the network detection block is a binary network mask it is necessary to fill the "holes". This is done by a applying a morphological filling over the mask (see Fig. 3).

### 3.1 Features Extraction

The vector of features extracted from each connected region is composed of features which characterize intensity, texture and shape, leading to a total of 51 features, which can be divided in two different groups:



**Fig. 3:** Output of the detection block: (left) original, with pigment network regions highlighted: (mid) output of the network detection block, (right) region mask after the morphological filling - each color represents a different region.

**(i) Image Features (38):** comprise information about intensity (histogram and variance) and texture (entropy and histogram of gradient). The histogram of intensities uses 26 bins, which consists in a total of 26 features. Entropy and variance are computed with the usual formulas, corresponding each one to one feature. The histogram of gradient (hog) is computed as follows [15]

$$hog_i = \sum_{(x,y)\in I(x,y)} G(x,y)\cdot b_i(\theta(x,y)) \tag{1}$$

where $G(x,y)$is the amplitude of the gradient of each region, $\theta(x,y)$is its direction and

$$b_i(\theta(x,y)) = \begin{cases} 1 & \text{if } \theta \in i\text{-th bin} \\ 0 & \text{if otherwise} \end{cases} \tag{2}$$

Gradient direction is quantified into 10 bins, with an angular interval of $18°$, leading to a total of 10 features.

**(ii) Topological Features (13):** this set of features characterize separately the structure of the"lines" and "holes". The "lines" are characterized by two features: network area and network area after applying a morphological erosion. Both areas are computed using the "lines" mask obtained by the network detection block. The "holes" and their structure are characterized by 11 features: number of holes and histogram of the area of holes , which consists of 10 features.

All features are normalized by using the area of the whole region (lines and holes).

### 3.2 Classification

A boosting algorithm (AdaBoost [14]) was used to discriminate pigment network regions from false alarms, since this kind of algorithms is capable of learning from classified data and has achieved remarkable results in challenging recognition problems. Moreover, it is also capable of performing a features' selecting process, which could provide interesting information in this specific problem. The classifier is trained by using a training set $\{(x_1,y_1),\ldots,(x_n,y_n)\}$, where $x_k \in \mathbb{R}^d$is a feature vector and $y_k \in \{0,1\}$is a binary label. Since the dataset contained more negative examples and different errors have different costs, different weights were given to the patterns

$$w_k = \begin{cases} \frac{\alpha}{m} & \text{if } y_k = 1 \\ \frac{1}{l} & \text{if } y_k = 0 \end{cases} \tag{3}$$

where $m$ is the number of positive examples, $l$ is the number of negative examples and $\alpha$ is a constant. Several values for $\alpha$

and the number of iterations $T$ and different features vectors were tested and the best combination was selected.

# 4 Lesion Classification

The previous block classifies the regions detected in the image as having a pigment network or not. However it is also necessary to assign a label to a binary image stating wether or not there is pigment network visible in it. Pigment network is a dense structure, which distributes more or less regularly throughout a lesion [1]. Assuming that, a binary lesion classification algorithm based on an area ratio was developed:

$$\lambda = \frac{A(R)}{A(L)} \tag{4}$$

where $A(R)$ is the area of the region $R$ originated from the union of all the detected and validate regions $R_i$ and $A(L)$ is the area of the segmented lesion $L$. $R$ is defined as the final binary network mask, the "holes" are not considered in this ratio.

A lesion is classified as *having pigment network* if $\lambda \geq T_A$ and *without pigment network* otherwise. $T_A$ is an empirically determined threshold.

# 5 Performance Metrics

Since the available data was limited, a 5-fold cross validation was used. Three different algorithms are evaluated in these results: region detection, AdaBoost and lesion classification algorithms. Their performance is assessed by computing the following figures of merit:

**(i) Region Matching:** The detection system (see Fig.2) provides a tentative set of pigment network regions. To assess the output of this system, a comparison with the ground truth segmentation of pigment regions $G_T$ is required. This involves a matching operation between the binary mask of detected regions $B_N$ and the ground truth which can be done as suggested in [16]. Each detected region can be classified as Correct Detection (CD) if the detected region matches one or more regions in $G_T$, False Alarm (FA) if the detected region has no correspondence or Detection Failure (DF) if one ground truth region has no correspondence. The three classes can be obtained by computing a correspondence matrix $C$. Considering that $G_T$ is composed of $P$ regions and that $B_N$ contains $M$ detected regions, $C$ is defined by

$$C(i,j) = \begin{cases} 1 & \text{if } A(B_{N_j} \cap G_{T_i}) \geq 0.7A(B_{N_j}) \\ & \qquad \forall\, i \in \{1,\ldots,\mathrm{P}\}, j \in \{1,\ldots,\mathrm{M}\} \\ 0 & \text{if otherwise} \end{cases} \tag{5}$$

where $A(B_{N_j} \cap G_{T_i})$ is the area of the region $B_{N_j} \cap G_{T_i}$ and $A(B_{N_j})$ is the area of $B_{N_j}$.

**(ii) Sensitivity (SE) and Specificity (SP):** these statistics are used to evaluate the performances of two blocks: the validation one, i.e., the performance of the AdaBoost algorithm regarding the classification of regions, and the lesion classification block.

# 6 Results and Discussion

The algorithm was tested is a dataset of 57 dermoscopy images, 13 with pigment network, extracted from the database of Hospital Pedro Hispano-Matosinhos. These were *rgb* images, stored in *bitmap* and *jpeg* formats, acquired during clinical exams using a dermatoscope with a magnification of 20x.

For each image a ground truth was extracted. First, each one of them was classified regarding the presence of pigment network (ground truth label), and for the ones where there is pigment network, the corresponding regions were manually segmented (ground truth region $G_T$). For training purposes a label was given to each one of the regions detected by the network detection block (see Fig. 2). Since there were regions partially occupied by pigment network,the labeling process was performed by imposing two different thresholds. Only regions containing more than 70% of the pigment network area, when compared with the region ground truth, were given the label 1, whereas other regions with less than 30% of the pigment network area were given the label 0. Regions with pigment network areas comprised in the interval 30%-70% were discarded.

Table 1 synthesizes the performance of AdaBoost for several values of $\alpha \in \{1, 3, 5, 10, 15\}$ and different combinations of features using a large number of iterations ($T = 2000$).

**Table 1:** Statistical results for the validation step using different $\alpha$ values. SE-sensitivity; SP-specificity.

| | Image Features | | Topological Features | | Both | |
|---|---|---|---|---|---|---|
| $\alpha$ | SP | SE | SP | SE | SP | SE |
| 1 | 78% | 30% | 80% | 44% | 82% | 38% |
| 3 | 74% | 35% | 79% | 45% | 78% | 42% |
| 5 | 73% | 36% | 76% | 45% | 77% | 42% |
| 10 | 71% | 37% | 76% | 46% | 76% | 45% |
| 15 | 70% | 39% | 75% | 47% | 74% | 45% |

By analyzing the results obtained, it was decided that the best combination of parameters for obtaining a good classification function should be $\alpha = 15$ and the use of topological features. Next, the best number of iterations $T$ for this problem was determined using $\alpha = 15$. It was found that $T = 100$ led to the best results. With $\alpha = 15$, $T = 100$ and topological features, the boosting algorithm achieves a $SE = 86\%$ and a $SP = 51\%$. A combination of parameters which leads to a high $SE$, despite the $SP$ value, was favored since it is assumed that a correct classification of pigment network regions is more important. From this point on, all the results were obtained using these values.

Fig. 4 illustrates the behavior of the detection algorithm for some images with pigment network. On the left the original image is shown, in the middle the output of the network detection block and on the right it is shown the output after the validation block. These results and the statistical ones shown in Table 2 show that the algorithm performs well and that the network detection is not compromised by applying a validation block, achieving 13 CD against only 3 DF after the validation step. The validation block allows a considerable

reduction in the number of FA (from 53 to 27).

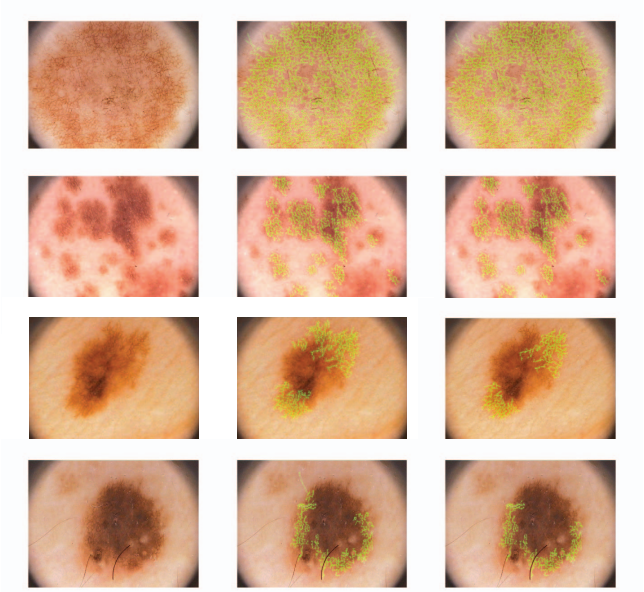


**Fig. 4:** Detection system results: (left) original: (mid) output of the network detection block, (right) final output after validation.

The small increasing in the number of DF after validation was expected, since the classifier does not have a $SE = 100\%$.

**Table 2:** Performance of the network detection system before and after the validation step using region matching. CD-Correct Detection; FA-False Alarm and DF-Detection Failure.

| | Before Validation | After Validation |
|---|---|---|
| CD | 15 | 13 |
| FA | 53 | 27 |
| DF | 1 | 3 |

Table 3 shows the overall performance of the lesion classification algorithm before and after the validation step. The threshold $T_A$ imposed was 0.1, i.e., 10% of the area of the lesion.

**Table 3:** Statistical results for the lesion classification algorithm before and after the validation step. SE-sensitivity; SP-specificity.

| | Before Validation | After Validation |
|---|---|---|
| SE | 85% | 78% |
| SP | 63% | 77% |

These results reinforce the importance of applying a validation block, since the $SP$ of the algorithm increased, which suggests a reduction in the number of wrongly classified lesions. The decreasing in the $SE$ value might be explained by the increasing in the number of DF. Nevertheless, the validation step significantly improves the the performance of the system.

# 7 Conclusions

This paper presents a method for the detections of pigment network in dermoscopic images. The proposed method extends the algorithm described in [9] by including a region validation step trained from classified data and a binary lesion classification. The proposed algorithm significantly reduces the number of false positives obtaining SE=78% and SP=77% in the detection of pigment network.

Future work should validate these results by using a larger database of classified images and should consider other types of features, including color texture features.

# 8 References


[1] "Dermoscopy tutorial," `http://www.dermoscopy.org/atlas/base.htm`.

[2] W. Stolz and *et al.*, "ABCD rule of dermatoscopy: a new practical method for early recognition of malignant melanoma.," *European Journal Dermatology*, , no. 4, pp. 521–527, 1994.

[3] G. Argenziano and *et al.*, "Epiluminescence microscopy for the diagnosis of doubtful melanocytic skin lesions. comparison of the ABCD rule of dermatoscopy and a new 7-point checklist based on pattern analysis.," *Archives of Dermatology*, , no. 134, pp. 1563–1570, 1998.

[4] S.W. Menzies and *et al.*, "Frequency and morphologic characteristics of invasive melanomas lacking specific surface microscopic features.," *Archives of Dermatology*, , no. 132, pp. 1178–1182, 1996.

[5] J. Mayer, "Systematic review of the diagnostic accuracy of dermatoscopy in detecting malignant melanoma," *Medical Journal Australia*, , no. 167, pp. 206–210, 1997.

[6] M. Binder and *et al*, "Epiluminescence microscopy of small pigmented skin lesions : short-term formal training improves the diagnosis performance of dermatologists.," *Journal American Academy of Dermatology*, pp. 197–202, 1997.

[7] G. Betta and *et al.*, "Dermoscopic image-analysis system: estimation of atypical pigment network and atypical vascular pattern," in *International Workshop on Medical Measurement and Applications*, April 2006.

[8] M. Sadeghi and *et al.*, "A novel method for detection of pigment network in dermoscopic imagesusing graphs," *Computerized Medical Imaging and Graphics*, , no. 35, pp. 137–143, 2011.

[9] C. Barata, J.S. Marques, and J. Rozeira, "Detecting the pigment network in dermoscopy images: a directional approach," in *33rd Annual International Conference on the IEEE EMBS*, IEEE, Ed., September 2011, pp. 5120–5123.

[10] C. Grana and *et al.*, "Line detection and texture characterization of network patterns.," in *In ICPR'06: Proceedings of the 18th International Conference on pattern Recognition*, 2006.

[11] M. Anantha and *et al.*, "Detection of pigment network in dermatoscopy images using texture analysis," *Computarized Medical Imaging and Graphics*, vol. 28, no. 5, pp. 225–234, 2004.

[12] M. Celebi and *et al.*, "Automatic detection of blue-white veil and related structures in dermoscopy images," *Computerized Medical Imaging and Graphics*, vol. 32, pp. 670–677, 2008.

[13] G. Fabbrocini and *et al.*, "Epilluminescence image processing for melanocytic skin lesion diagnosis based on 7-point check list: a preliminary discussion on three parameters," *The open dermatology journal*, vol. 4, pp. 110–115, 2010.

[14] P. Viola and M. Jones, "Robust real-time face detection," *International Journal of Computer Vision*, vol. 57, no. 2, pp. 137–154, 2004.

[15] N. Dalal and B. Triggs, "Histogram of oriented gradients for human detection.," in *CVPR*, IEEE, Ed., 2005, vol. 1, pp. 886–893.

[16] J. C. Nascimento and J. S. Marques, "Novel metrics for performance evaluation of object detection algorithms," in *Sixth IEEE International Workshop on Performance Evaluation of Tracking and Surveillance*, IEEE, Ed., May 2004.